ORIGINAL ARTICLE

Influence of fixed abrasive configuration on the polishing process of silicon wafers

Congfu Fang[1] · **Zaixing Zhao**[1] · **Longyuan Lu**[1] · **Yanfen Lin**[2]

Abstract Lapping and polishing with fixed abrasives is an efficient method to flatten wafers and obtain mirror surface finish. One of the most concerned things is abrasive configuration for polishing pads in research. Researching on pad's abrasive configuration will help get better wafer surface quality. For abrasive trajectories can heavily affect wafer surface flatness and roughness during lapping and polishing process, the present work was conducted to study the relationship among abrasive configuration, trajectory distribution, material removal, and its influence on wafer surface quality. For this purpose, an abrasive configuration method was applied by adopting a written Matlab program to give set values of the radial distance and the initial angle of abrasives fixed on the pad surface. Based on the method, polishing pads with the regular and radial configurations were designed and used to study trajectory distributions under different polishing parameters. The polishing experiments were carried out on silicon wafers with the regular and the radial diamond polishing pads made by the sol-gel method. The wafer surface morphology, thickness, and roughness were detected in polishing. The results show that better flatness and roughness distributions can be obtained through using the radial pad than that of the regular pad, which is due to the smaller value of variation coefficient of the standard deviation for trajectory density and better global profile of trajectory density. The method of pad design and trajectory analysis can be an effective way to design pads with proper abrasive configurations for different applications in lapping and polishing process.

Keywords Wafer polishing · Abrasive configuration · Trajectory · Uniformity · Roughness

1 Introduction

Lapping and polishing with abrasives, as an important means of realizing precision and ultra-precision processing, can obtain excellent shape and dimensional accuracy of workpiece and is widely used in the processing of silicon, silicon carbide, sapphire, functional ceramic substrates, and other hard and brittle materials for industrial applications [1, 2]. With the rapid development of nanoelectronics, new materials science, and optoelectronic information industry, there is a much higher demand of planarization, uniformity, and controllability of process for lapping and polishing, especially for large diameter workpiece processing, as a result of kinematics and trajectories adopted for machining process [3].

In actual lapping and polishing process with free abrasives (CMP), the polishing result is determined by many factors such as kinematic parameters, slurry distribution, temperature distribution, stress distribution, and etc [4–6]. Therefore, several models based on the Preston equation, contact mechanism, abrasive scratch, and other effects have been proposed due to the combined action of the chemical and mechanical effects [7–10]. As the kinematic aspect is the most basic uniformity factor, many related calculations or simulations regarding the kinematic parameters of CMP tools have been performed. An attempt to investigate the effect of kinematics on uniformity in chemical mechanical planarization was conducted by Hocheng and Tso. It was found that the relative velocity is not constant [11, 12]. Kim et al. [13] further

✉ Congfu Fang
   cffang@hqu.edu.cn

1 College of Mechanical Engineering and Automation, Huaqiao University, Xiamen, Fujian 360121, China

2 School of Electronic, Electrical and Computer Engineering, Xiamen Institute of Technology University, Xiamen, Fujian 360121, China

proposed the concept of the sliding distance distribution and revealed that the basic kinematic parameters have a great influence on the non-uniformity. In order to clarify the influences of kinematics on surface quality, tool wear and optimization of process parameters, motion forms, and their trajectory equations for different lapping and polishing machines were investigated by scholars [14–17]. However, most studies were mainly focused on trajectories with a single abrasive grit; the results can be qualitatively obtained by artificial observation of the trajectory map and used to guide the optimal selection of processing parameters. In order to quantitatively reveal the influence of processing parameters on the trajectory distribution, Su et al. [2] followed those works and put forward the within-wafer-non-uniformity (WIWNU) of material removal to evaluate the trajectory distribution with 60 abrasive particles. The main idea of WIWNU was based on counting the number of the sliding trajectory points. The study results indicate that the rotational velocity ratio has an obvious influence on trajectory distributions. Those previous studies on kinematics and trajectories in CMP are mainly based on the mechanical action executed by the effective abrasive particles discretely embedded in pad asperities [18]. In effect, free abrasives in lapping and polishing have a random distribution and uncontrollable trajectory besides low efficiency, environmental pollution problems, and etc. Therefore, lapping and polishing with fixed abrasives was put forward, and it has many obvious advantages in terms of machining precision and efficiency for the controllable trajectory and abrasive distribution [19–21].

In lapping and polishing with fixed abrasives, an early study on lapping with fixed abrasives was conducted by Uhimann et al. [22], which was focused on the kinematics in the face grinding process on lapping machines, and indicates that the trajectory has a heavy influence on the workpiece surface flatness and roughness besides tool wear. In the aspect of abrasive configuration, Hon-Yuen et al. [23] focused on the study of kinematics based on two kinds of geometric arrangements, which were accordingly named of Delta and Ypsilon arrangements. The main goal was to evaluate the influence of the geometric-arranged abrasive tools on the material removal rate during polishing. It was found that the Ypsilon arranged tool is capable to provide higher material removal rate than that of the Delta arranged tool. In the grinding process of glass, Sousa et al. [24] adopted the two abovementioned abrasive tools to investigate the effects of kinematics and abrasive configurations, and also obtained the similar conclusions. Li et al. [25] investigated the influence of self-made symmetrical and spiral lapping disks, which were brazed with micro powder diamond in lapping of silicon wafer and alumina ceramic,

on the surface morphology, roughness, and removal rate in lapping. Regretfully, the effects of abrasive configurations on the trajectory distributions and the workpiece surface quality were not further analyzed in those studies. Recently, some researches have been mainly focused on pad wear and pad conditioning with fixed abrasive trajectory analysis besides experimental investigations in lapping and polishing process. Feng [26] analyzed different pad conditioning density distributions in CMP process, which were used polishing trajectories generated by a diamond dresser to analyze the pad wear rate. The results show that the influence of different patterns of abrasive distributions on conditioning density function is insignificant. Emmanuel et al. [27] adopted the genetic algorithm method to design optimization of diamond disk pad conditioner. Nguyen et al. [28] analyzed kinematic motions and the contact time to investigate the pad wear non-uniformity caused by the conditioner with fixed abrasives and found that the contact time has a heavy influence on the trajectory distribution.

Although those previous studies provided a nice basis to understand the influences of kinematics and trajectories during machining, few studies have yet reported the relationship among the abrasive configuration of polishing pads, trajectory distribution, and its influence on workpiece surface quality. The present paper was carried out based on the specific design and the analysis of the trajectory as a standard method; two abrasive configurations of polishing pads were designed. Through trajectory calculation and corresponding experimental investigations, the effects of abrasive configurations on trajectory distributions and wafer surface quality were further analyzed, which are of most importance to design and choose proper abrasive configurations for pads in lapping and polishing process in the pursuit of high workpiece surface quality.

2 Kinematic model of workpiece surface trajectory

Plane lapping and polishing with the rotary type are the most widely used polishers, which mainly consist of a polishing platen, workpiece carrier, and liquid delivery system shown in Fig. 1. The pad and the workpiece rotate in the same direction around their respective axes with the rotational speed ω_g and ω_w, respectively. To describe the trajectory of a fixed abrasive, two coordinate systems are defined shown in Fig. 2. A fixed coordinate system XOY is located at the pad center, and a workpiece coordinate system xoy is fixed at the carrier center. R is the pad radius and r is the workpiece radius. e is the distance from the pad center to the workpiece center, which is called eccentricity. Taken a typical contact point p, which refers to an abrasive grain fixed on the pad, into account, the
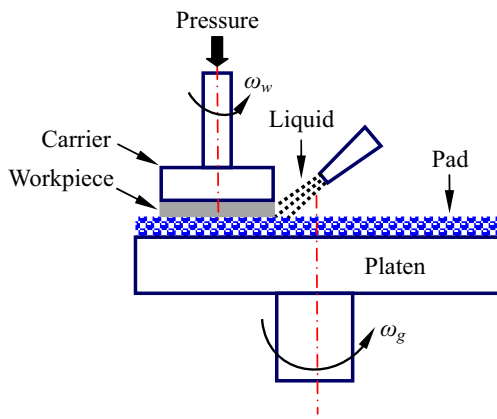
Fig. 1 The schematic diagram of polishing

distance from point p to the pad center is R_p, and the initial angle of point p is θ_p.

Based on the polishing kinematic model, the abrasive moving trajectory in the fixed coordinate system XOY can be described as follows:

$$\begin{bmatrix} X \\ Y \end{bmatrix} = \begin{bmatrix} R_p\cos(\theta_p + \omega_g t) \\ R_p\sin(\theta_p + \omega_g t) \end{bmatrix} \quad (1)$$

For the coordinate system xoy and the fixed coordinate system XOY have a translational relationship, which can be written as follows:

$$\begin{bmatrix} X \\ Y \end{bmatrix} = \begin{bmatrix} \cos(\omega_w t) & -\sin(\omega_w t) \\ \sin(\omega_w t) & \cos(\omega_w t) \end{bmatrix} \begin{bmatrix} x \\ y \end{bmatrix} + \begin{bmatrix} e \\ 0 \end{bmatrix} \quad (2)$$

Thus, the trajectory equation in XOY can be translated to the workpiece xoy system, which can be written as follows:

$$\begin{bmatrix} x \\ y \end{bmatrix} = \begin{bmatrix} \cos(\omega_w t) & \sin(\omega_w t) \\ -\sin(\omega_w t) & \cos(\omega_w t) \end{bmatrix} \left(\begin{bmatrix} R_p\cos(\theta_p + \omega_g t) \\ R_p\sin(\theta_p + \omega_g t) \end{bmatrix} - \begin{bmatrix} e \\ 0 \end{bmatrix} \right) \quad (3)$$
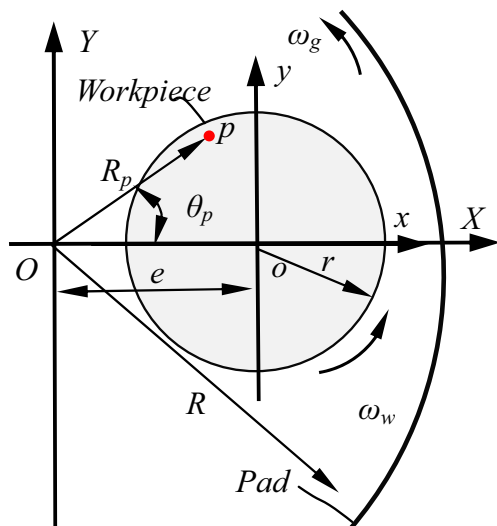

Fig. 2 The polishing kinematic model

Then, the trajectory of a contact point p can be expressed in the rotating (x_p, y_p) as follows:

$$\begin{cases} x_p = R_p\cos(\theta_p + \omega_g t - \omega_w t) + e\cos(\omega_w t) \\ y_p = R_p\sin(\theta_p + \omega_g t - \omega_w t) - e\sin(\omega_w t) \end{cases} \quad (4)$$

In order to conveniently analyze the influence of processing parameters on trajectory, the rotational speed ratio of the workpiece to the pad is defined as follows:

$$k = \frac{\omega_w}{\omega_g} \quad (5)$$

3 Calculation method of trajectory distribution

For trajectory analysis is a standard method to study the generation of workpiece's geometrical profile and to predict the processing accuracy, a calculation method of trajectory distribution is applied in the present paper. Firstly, the workpiece surface on which the trajectory is distributed is meshed to lots of small squares. The schematic of meshed small squares for workpiece surface is shown in Fig. 3. In this paper, the size of the meshed squares is 1 mm × 1 mm, and the corresponding time step is 0.001 s in order to obtain a precise trajectory distribution with the consideration of the whole process. Next, the number of trajectories n_i as well as its scratching area s_i distributed in the ith meshed square on the workpiece surface is calculated according to the coordinate of trajectory point [2, 29].

Then, the density of trajectory distribution in each square region is calculated, and it can be expressed as follows:

$$\rho_i = n_i/s_i \qquad (i = 1, 2, \cdots N) \quad (6)$$

where n_i is the number of scratches in ith square. s_i is the area of ith square. ρ_i is the density of trajectory on ith square. N is the total number of all squares meshed on the workpiece surface.
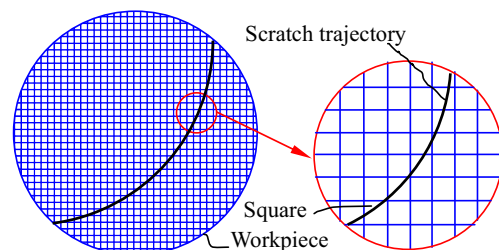

Fig. 3 Schematic of the meshed small squares on workpiece

Based on the density of trajectory distribution, the standard deviation (SD) of all values of density ρ_i can be expressed as follows:

$$SD = \sqrt{\frac{\sum_i^N \left(\rho_i - \overline{\rho}\right)^2}{N-1}} \qquad (i = 1, 2, \cdots N) \qquad (7)$$

where $\overline{\rho}$ is the average density of all values of density ρ_i.

At last, for the average density $\overline{\rho}$ is much different under different process parameters, simulation time, the number of abrasives located on the pad, and the abrasive distribution, it is important to analyze the distribution of trajectory under the same level for different conditions. Therefore, the variation coefficient of SD (VCSD) is applied to evaluate the global trajectory distribution on the workpiece surface, and it can be written as follows:

$$VCSD = SD/\overline{\rho} \qquad (8)$$

The smaller value of VCSD means the better trajectory distribution on the workpiece surface, which is more helpful to improve the accuracy of the workpiece surface and obtain proper patterns of polishing pads.

4 Polishing pad design and trajectory analysis

4.1 Pads designed with different abrasive configurations

Based on Eq. (4), it can be found that abrasive trajectories generated by a polishing pad can be easily obtained with given set values of the abrasive radial distance and the initial angle (R_p, θ_p) besides polishing parameters. For Maltlab software has the advantages of matrix operations and scientific drawing, polishing pads can be designed with Matlab software, and matrix can be used to refer the position information of
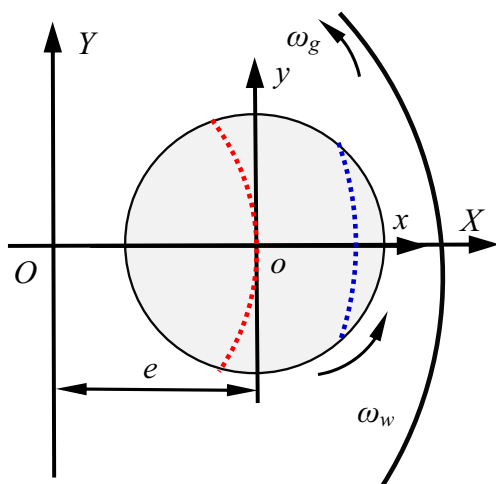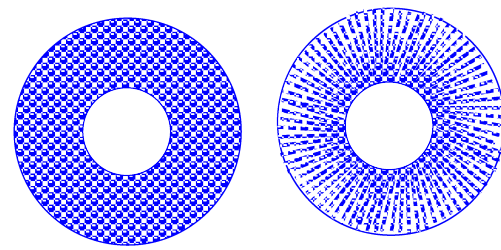

Fig. 4 The effect of abrasive position

(a) Regular   (b) Radial

Fig. 5 Illustration of pads with different patterns

abrasives located at the pad surface. For the path of abrasive scratches on the workpiece surface is determined by the abrasive position besides process parameters shown in Fig. 4. It can be seen that the number of abrasives scratching on the workpiece center is more than that scratching on the workpiece edge. Taken the influence of abrasive position into account, two patterns of abrasive distributions are used to pad design in the present paper, one is the regular configuration which is often used in lapping and polishing and the other one is the radial configuration which is designed to reduce the number of abrasives scratching on the workpiece center. The illustration of pads with the regular and the radial configurations is shown in Fig. 5.

Taken the actual lapping and polishing process into account, there are numerous abrasives fixed in the pad, and abrasives are hard to distinguish with the naked eyes. Therefore, it is necessary to analyze trajectory distribution statistically. For the number of abrasives is more than 1,000, 000 in an actual lapping and polishing process according to the studies of Uneda et al. [30–32], it is impractical to calculate trajectory distribution based on this number due to many time steps and meshed small squares involved. Therefore, in order to guarantee the calculation precision and computational efficiency [16, 28], the number of abrasives is about 12,000 abrasives for both regular and radial pads. The pad diameter is 280 mm, which is identical with the pads used in the following experiments. Though using a written Matlab program,
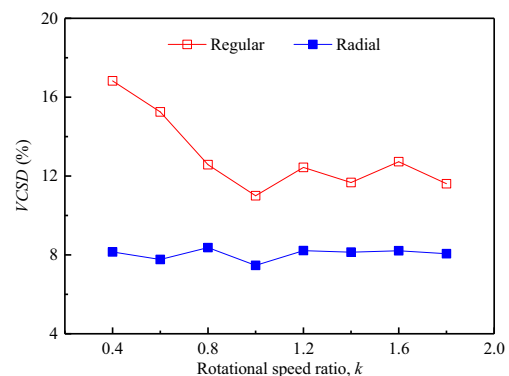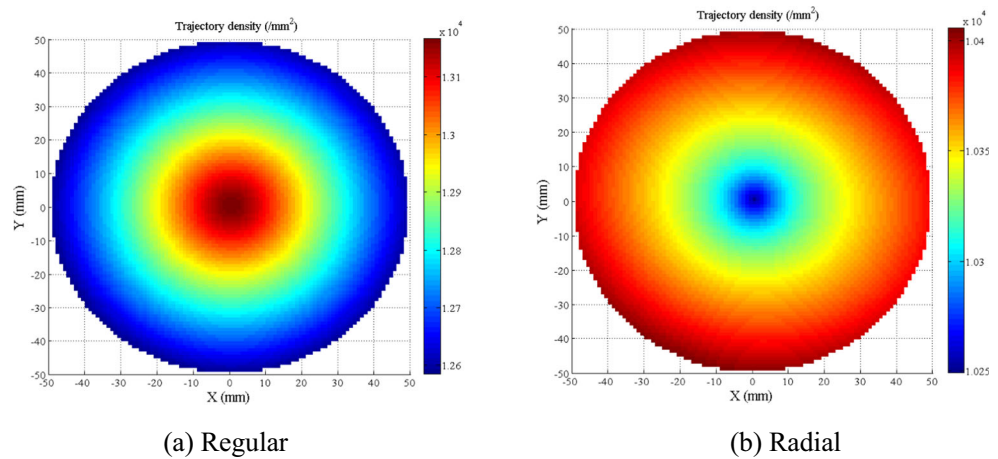

Fig. 6 Calculated results of VCSD with the regular and radial pads

Fig. 7 Calculated profiles of trajectory density with the regular and radial pads

(a) Regular   (b) Radial

abrasives are arranged with isometric array for the regular pad and are arranged 80 radial directions for the radial pad.

4.2 Trajectory analysis

Based on Eqs. (4) and (8), the abrasive trajectory distribution can be calculated using Matlab software. For the rotational speed ratio has a heavy influence on trajectory distributions, the trajectory distributions caused by the regular and the radial pads were analyzed under different rotational speed ratios. In calculation, for the abrasive radial distance and the initial angle (R_p, θ_p) can be obtained during abrasive configuring based on the written Matlab program. Therefore, taking the workpiece diameter $r = 100$ mm, the certain eccentric distance $e = 100$ mm, the workpiece rotational speed $\omega_g = 60$ rpm, and simulation time is 10,000 steps, the results of VCSD for the global trajectory distributions with two pads are shown in Fig. 6.

As shown in Fig. 6, it can be seen that the rotational speed ratio indeed has an obvious influence on the global trajectory distributions in both regular and radial configurations, but the effects of the rotational speed ratio are much different from each other. The influence of the rotational speed ratio on the regular pad is much heavily than that on the radial pad. From Fig. 6, it can be found that the values of VCSD are ranged from about 10.8 to 17.1 % for the regular configuration, but from about 7.7 to 8.6 % for the radial configuration. According to the literature [33], the trajectory distribution is affected by the radial distance and the initial angle of fixed abrasives, but the shape of trajectory is not changed with the initial angle. Therefore, the influence of the radial configuration is much slight than that of the regular configuration. Based on Fig. 6, it can be concluded that better flatness could be obtained in polishing with the radial configuration pad for its smaller values of VCSD.

Although the value of VCSD can be only used to reflect the global uniformity of trajectory distribution, the profile of trajectory density cannot be revealed. For roughness is related to the number of abrasive scratches on the workpiece surface, more scratches can help obtain lower surface roughness. Therefore, the trajectory density profiles were plotted under the rotational speed ratio $k = 1$ shown in Fig. 7. It can be seen that the global trajectory density caused by two pads is much different. The lower average roughness could be gained from the regular pad than that of the radial pad for the higher global trajectory density. However, the trajectory density distributions for two pads are much different from each other; the trajectory density tends to be a convex distribution with the regular pad, but it tends to be a concave distribution with the radial pad, which basically indicates that the roughness distribution on the workpiece surface is much different.

It should be mentioned that the most reasonable rotational speed ratio for the regular and the radial configurations is different based on Fig. 6, but the rotational speed ratio can be selected from 0.8 to 1.2 for both abrasive configuration pads with the consideration of proper rotational speed ratio adopted in effect. In following experiments, the rotational speed ratio $k = 1$ was selected in order to compare the effects of two configuration pads on the polishing results.

5 Experimental set-up

According to the polishing pads designed above, two polishing pads (diameter 280 mm) based on the regular and

Table 1 Fabrication conditions of the polishing pads

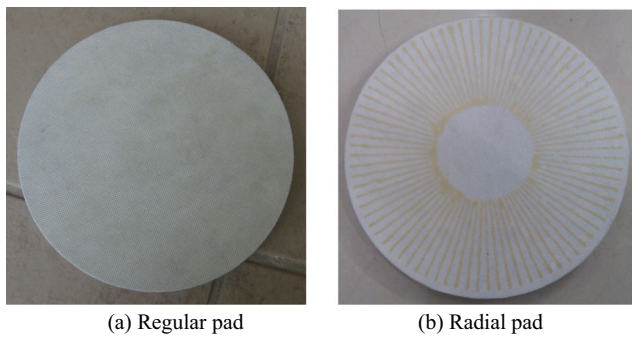| Diamond size, μm	Diamond concentration, wt%	Film thickness, mm	Gelling reaction time, min	Drying time, min
w40	5	0.3	60	120

(a) Regular pad   (b) Radial pad

Fig. 8 Polishing pads fabricated with different patterns

Fig. 9 Illustrations of the experimental set-up

radial configurations were made by the sol-gel method. In fabrication, polishing pads containing diamond abrasives with grit size of 40 μm were fabricated through four procedures including mixing, screeding, gelling, and drying. Fabrication conditions of the polishing pads were shown as follows: diamond abrasive concentration was 5 wt%, thickness of the polishing film 0.3 mm, gelling reaction time of 60 min, and drying time of 120 min, which is shown in Table 1. The polishing pads fabricated by the sol-gel method are shown in Fig. 8.

The workpiece used in the experiments is silicon wafers with the diameter of 76 mm; the original silicon wafer surface roughness was 0.145 μm. The main performance parameters of the silicon wafer are shown in Table 2.

Based on the silicon wafer workpiece and the self-made polishing pads, the polishing experiments were conducted on an AUTOPOL-1000S lapping and polishing machine shown in Fig. 9. In the experiments, the rotational velocity of silicon and polishing pad was fixed at 60 rpm, respectively, pressure was 1.5 kg, polishing time was 90 min, and distilled water was utilized as the coolant. The polishing parameters adopted in the experiments are shown in Table 3.

To obtain the influence of the two polishing pads on the surface quality of silicon wafers, the surface morphologies were observed by a VHX-1000 optical microscope. The wafer thicknesses were measured by the thickness gauge at 20 different positions in order to obtain the profile of thickness distribution. The surface roughnesses were measured by Mahr XR20 at six different positions in order to obtain the profile of roughness distribution. It should be mentioned that the surface morphologies, thicknesses, and roughnesses of silicon wafers were detected at the beginning and end of the experiments, respectively.
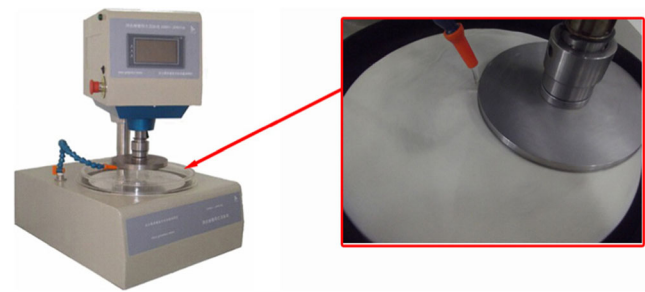
6 Results and discussion

The surface morphologies of silicon wafers in polishing with the regular polishing pad and the radial polishing pad are shown in Table 4.

Based on Table 4, it can be observed that many light spots occurred in the fringe area of the silicon wafers after polishing either with the regular pad or with the radial pad, but it is much different in the central area of the silicon wafers. In the regular pad polishing, few spots occurred in the center area of the wafer except the fringe area; the wafer surface seems to be smoother in the center area than that in the fringe area. In the radial pad polishing, spots occurred either in the wafer center area or the wafer fringe area, but the number of spots occurred in the wafer center area is relatively less than that in the wafer fringe area; the wafer surface seems to be relatively smoother in the center area than that in the fringe area. Therefore, it can be found that the morphology difference in the radial pad polishing is smaller than that in the regular pad polishing, which indicates that the material seems to be removed more uniformly when polishing with the radial pad than that with the regular pad; the big difference is mainly due to the different trajectory density distribution shown in Fig. 7. As shown in Fig. 7, the trajectory density ranges from about 1.26×10^4 mm^{-2} in the wafer fringe to about 1.32×10^4 mm^{-2} in the wafer center in the regular pad polishing, but it ranges from about 1.025×10^4 mm^{-2} in the wafer center to about 1.04×10^4 mm^{-2} in the wafer fringe in the regular pad polishing. The results indicate that polishing with the radial pad can obtain more uniform workpiece surface for much less trajectory density variation, and it is basically consistent with the wafer morphology results. In order to further clarify the difference, the thicknesses of the silicon wafers were measured before and after polishing shown in Fig. 10.

As shown in Fig. 10, the values of wafer thickness undulations after polishing with the regular pad are bigger than that with the radial pad. The thickness variation is about 2.8 μm in polishing with the regular pad, but it is about 1.8 μm in polishing with the radial pad, which indicates that the material removal is more uniform when polishing with the radial pad than that with the regular pad. So, it is easier to get better flatness when polishing with the radial pad. The results reveal

Table 2 Main performance parameters of silicon wafer

Mohs hardness	Density, g/cm^3	Young's modulus, Gpa	Fracture toughness, Mpa.m$^{1/2}$
7	2.33	187	0.68

Table 3 Machining parameters in polishing of silicon wafer

Wafer rotational velocity, r/min	Pad rotational velocity, r/min	Certain eccentric distance, mm	Polishing pressure, kg	Polishing time, min
60	60	100	1.5	90

the heavy influence of abrasive configuration on the wafer flatness; the smaller value of VCSD can achieve the better flatness, which shows a good agreement with the analytical results shown in Fig. 6.

Based on Fig. 10, it can be found that the average removal thickness of silicon wafer in polishing with the regular pad is about 10.2 μm, and it is about 9.8 μm in polishing with the radial pad, which indicates that the removal rate in the radial pad polishing is slightly lower than that in the regular pad polishing. To reveal the difference of material removal, the removal thicknesses of silicon wafers in polishing with different pads are shown in Fig. 11. It can be seen that the wafer material removal in the wafer center is greater than that on the wafer edge when polishing with the regular pad, but the results are in contrast when polishing with the radial pad. According to the profile of trajectory density shown in Fig. 7, it can be found that the profile of the removal thickness is generally similar to the profile of trajectory density either with the regular pad or with the radial pad, which proves that the profile of trajectory density has an obvious influence on material removal and finally further influences the wafer flatness.

Figure 12 shows the roughnesses of silicon wafers in the different positions. It can be found that the value of the average surface roughness is about 0.024 μm in polishing with the

regular pad, but it is about 0.027 μm in polishing with the radial pad. The value of the average roughness with the regular pad is lower than that with the radial pad, which has a good agreement with the analytical results for higher global trajectory density with the regular pad. But, there is a big difference in the roughness distributions for two silicon wafers with different pads. In polishing with the regular pad, roughness near the wafer center is much smaller than that near the wafer edge. But in polishing with the radial pad, roughness near the wafer center is relatively close to that near the wafer edge. The polishing results have a basically agreement with the results based on the profile of trajectory density in polishing with the regular pad shown in Fig. 7, but it has much different in polishing with the radial pad. The main reason is probably due to the pressure on the contact interface of the polishing pad and the workpiece. Hertz contact theory is used in traditional lapping and polishing process [34], but it is not suitable for pads with fixed abrasives. Recently, Dong et al. have found that the marginal pressure is about 75 % of center pressure; the pressure distribution tends to be a convex distribution, and its curves can be fitted by polynomial in lapping and polishing with fixed abrasives [35]. Based on the results of Dong's study, it can be concluded that the actual profile of trajectory density can be influenced by the weight of pressure

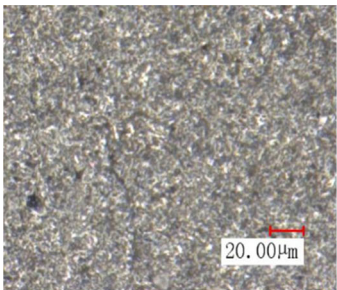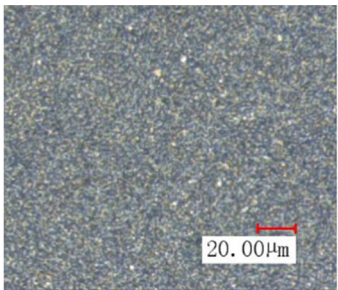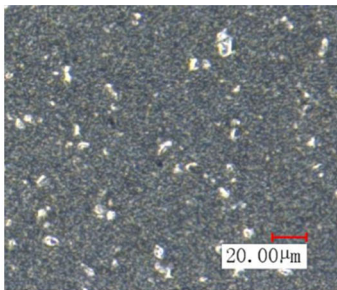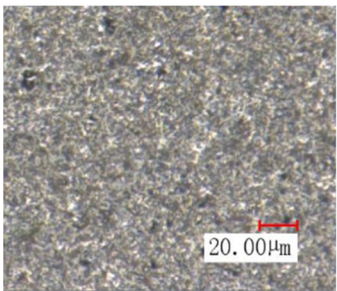**Table 4** Silicon wafer surface morphologies in polishing with different pads
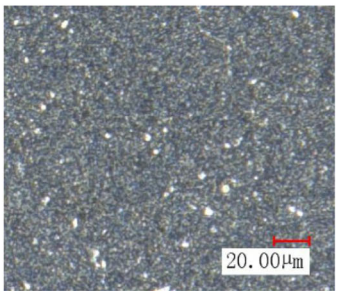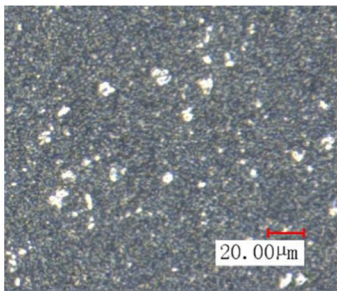
Fig. 10 Wafer thickness before and after polishing with different pads

(a) Polishing with the regular pad

(b) Polishing with the radial pad
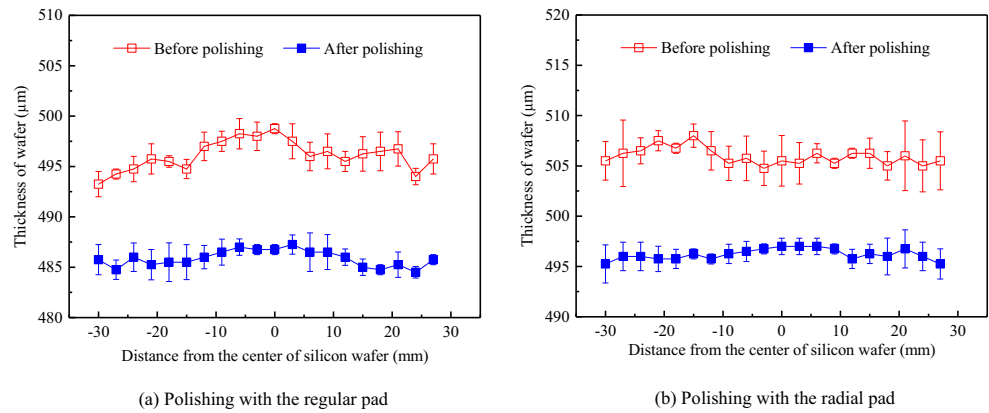
distribution, and it will further affect the surface roughness distribution. Taken the influence of the convex pressure distribution into account, it can be found that the convex profile of trajectory density distribution with the regular pad can be aggravated, and it results in a bigger difference between the workpiece center and the workpiece edge; the weight profile of trajectories tends to be more convex. But for the radial pad, the concave profile of trajectory density distribution is weakened, and it reduces the difference between the workpiece center and the workpiece edge; the weight profile of trajectories tends to be uniform. Hence, it is not hard to understand that the difference of roughness distribution on the wafer surface is obvious in polishing with the regular pad, but it is not obvious in polishing with the radial pad.

Based on the above analysis, it can be concluded that the material removal and wafer surface quality is greatly dependent on the trajectory distribution, which is further affected by the pad's abrasive configuration. Therefore, it is of significance to design pads with proper abrasive configuration in the pursuit of high workpiece surface quality. Based on the method of pad design and trajectory analysis put forward in the present work, pads with reasonable abrasive configurations can be effectively designed for different applications in lapping and polishing process.

7 Conclusions

In order to reveal the influence of abrasive configuration on trajectory distribution, material removal, and wafer surface quality, the method of pad design and corresponding trajectory analysis was put forward in the present paper; trajectories caused by pads with different abrasive configurations can be readily calculated and analyzed. It is found that abrasive configuration has an obvious influence on trajectories under different rotational speed ratio. Pads with different abrasive configurations can lead to different values of VCSD and trajectory profiles, which will further influence the material removal, flatness, and surface roughness.

Based on the results of wafer polishing experiments with the regular and radial pads, the results show that better flatness and roughness distribution can be obtained with the radial pad. Through comparing with the corresponding calculated trajectory results, it is found that the flatness of the wafer is basically determined by the value of VCSD when using pads with different patterns, the smaller value of VCSD can achieve better flatness in polishing. The profile of trajectory density distribution with specific pads could reveal the roughness distribution, especially taken the pressure into account; the higher global trajectory density can obtain smaller value of average surface roughness under the same number of abrasives.
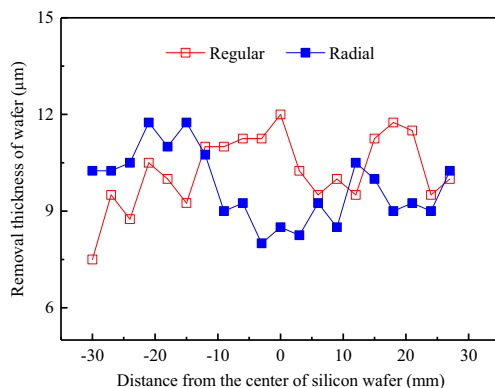

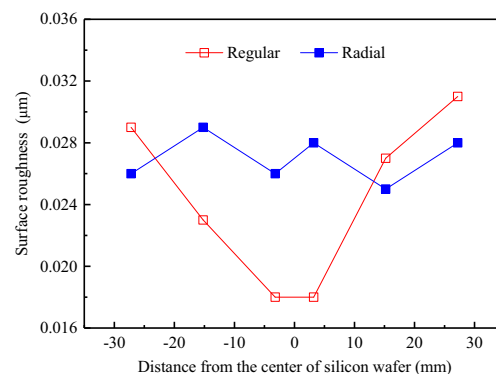**Fig. 11** Removal thickness with different pads

Fig. 12 Roughness with different pads

With the method of pad design and corresponding trajectory analysis put forward in the present paper, pads with different abrasive configurations can be further simulated based on the *VCSD* as the evaluation index; more reasonable abrasive configuration pads can be designed though computational simulations for different applications in lapping and polishing process.

References

1. Yuan JL, Wang ZW, Wen DH, Lu BH, Dai Y (2000) Review of the current situation of ultra-precision machining. Chin J Mech Eng 43(1):35–48

2. Su JX, Guo DM, Kang RK, Jin ZJ, Li XJ, Tian YB (2004) Modeling and analyzing on nonuniformity of material removal in chemical mechanical polishing of silicon wafer. Mater Sci Forum 471–472:26–31. doi:10.4028/www.scientific.net/MSF.471-472.26

3. Sousa FJP, Aurich JC, Weingaertner WL, Alarcon OE (2007) Kinematics of a single abrasive particle during the industrial polishing process of porcelain stoneware tiles. J Eur Ceram Soc 10:3183–3190. doi:10.1016/j.jeurceramsoc.2006.12.007

4. Shan L, Levert J, Meade L, Tichy J, Danyluk S (1999) Interfacial fluid mechanics and pressure prediction in chemical mechanical polishing. J Tribol 122(3):539–543. doi:10.1115/1.555398

5. Wang CL, Jin ZJ, Kang RK (2008) Effects of kinematic forms on material removal rate and non-uniformity in chemical mechanical planarisation. Int J Mater Prod Technol 31:54–62. doi:10.1504/IJMPT.2008.015895

6. Oh S, Seok J (2008) Modeling of chemical-mechanical polishing considering thermal coupling effects. Microelectron Eng 85(11):2191–2201. doi:10.1016/j.mee.2008.04.037

7. Zhao YW, Chang L, Kim SH (2003) A mathematical model for chemical-mechanical polishing based on formation and removal weakly bonded molecular species. Wear 254(3-4):332–339. doi:10.1016/S0043-1648(03)00015-2

8. Castillo-Mejia D, Beaudoin S (2003) A locally relevant prestonian model for wafer polishing. J Electrochem Soc 150(2):96–102. doi:10.1149/1.1532330

9. Bozkaya D, Muftu S (2009) A material removal model for CMP based on the contact mechanics of pad, abrasives and wafer. J Electrochem Soc 156(12):890–902. doi:10.1149/1.3231691

10. Bott S, Rzehak R, Vasilev B, Kucher P, Bartha JW (2011) A CMP model including global distribution of pressure. IEEE Trans Semicond Manuf 24(2):304–314. doi:10.1109/TSM.2011.2107532

11. Hocheng H, Tsai HY, Tsai MS (2000) Effects of kinematic variables on non-uniformity in chemical mechanical planarization. Int J Mach Tools Manuf 40:1651–1669. doi:10.1016/S0890-6955(00)00013-4

12. Tso PL, Wang YY, Tsai MJ (2001) A study of carrier motion on a dual face CMP machine. J Mater Process Technol 116:194–200. doi:10.1016/S0924-0136(01)01045-7

13. Kim HJ, Jeong HD (2004) Effect of process conditions on uniformity of velocity and wear distance of pad and wafer during chemical mechanical planarization. J Electron Mater 33(1):53–60. doi:10.1007/s11664-004-0294-4

14. Yang JD, Wen XH, Zhu YQ, Wang LJ (1997) Discussing on solid abrasive lapping path. Chin J Mech Eng 10(2):101–105

15. Pan JS, Yan QS, Xu XP, Zhu JT, Wu ZC, Bai ZW (2012) Abrasive particles trajectory analysis and simulation of cluster magnetorheological effect plane polishing. Phys Procedia 25(22):176–184. doi:10.1016/j.phpro.2012.03.067

16. Zhao DW, Wang TQ, He YY, Lu XC (2013) Kinematic optimization for chemical mechanical polishing based on statistical analysis of particle trajectories. IEEE Trans Semicond Manuf 26(4):556–563. doi:10.1109/TSM.2013.2281218

17. Yuan JL, Yao WF, Zhao P, Lyu BH, Chen ZX, Zhong MP (2015) Kinematics and trajectory of both cylindrical lapping process in planetary motion type. Int J Mach Tools Manuf 92:60–71. doi:10.1016/j.ijmachtools.2015.02.004

18. Luo JF, Dornfeld DA (2003) Effects of abrasive size distribution in chemical mechanical planarization: modeling and verification. IEEE Trans Semicond Manuf 16(3):469–476. doi:10.1109/TSM.2003.815199

19. Zuo DW, Sun YL, Zhao YF, Zhu YW (2009) Basic research on polishing with ice bonded nanoabrasive pad. J Vac Sci Technol B 27(3):1514–1519. doi:10.1116/1.3125272

20. Zarudi I, Zhang L (1996) Subsurface damage in single-crystal silicon due to grinding and polishing. J Mater Sci Lett 15:586–587. doi:10.1007/BF00579258

21. Tateishi T, Gao Q, Tani Y, Yanagihara K, Sato H (2006) Development of a high-porosity fixed abrasive pad utilizing catalytic effects of TiO2 on polyurethane matrix. CIRP Ann Manuf Technol 55(1):321–324. doi:10.1016/S0007-8506(07)60426-0

22. Uhlmann E, Ardelt T, Spur G (1999) Influence of kinematics on the face grinding process on lapping machines. Ann CIRP 48(1):281–284. doi:10.1016/S0007-8506(07)63184-9

23. Tam HY, Cheng HB (2010) An investigation of the effects of the tool path on the removal of material in polishing. J Mater Process Technol 210(5):807–818. doi:10.1016/j.jmatprotec.2010.01.012

24. Sousa FJP, Hossea DS, Reichenbach I, Aurich JC, Seewig J (2013) Influence of kinematics and abrasive configuration on the grinding process of glass. J Mater Process Technol 213:728–739. doi:10.1016/j.jmatprotec.2012.11.026

25. Li QC, Shen JY, Fang CF, Xu XP (2014) Study on fixed abrasive lapping hard and brittle materials with brazed micro powder diamond disk. Key Eng Mater 589–590:451–456. doi:10.4028/www.scientific.net/KEM.589-590.451

26. Feng T (2007) Pad conditioning density distribution in CMP process with diamond dresser. IEEE Trans Semicond Manuf 20(4):464–475. doi:10.1109/TSM.2007.907618

27. Baisie EA, Li ZC, Zhang XH (2013) Design optimization of diamond disk pad conditioners. Int J Adv Manuf Technol 66:2014–2052. doi:10.1007/s00170-012-4480-x

28. Nguyen NY, Zhong ZW, Tian Y (2015) An analytical investigation of pad wear caused by the conditioner in fixed abrasive chemical-mechanical polishing. Int J Adv Manuf Technol 77:897–905. doi:10.1007/s00170-014-6490-3

29. Spur G, Eichhorn H (1997) Kinematisches Simulationsmodell des lappscheibenverschleiβes. IDR 31(2):169–178

30. Yeruva SB, Park CW, Rabinovich YI, Moudgil BM (2009) Impact of pad-wafer contact area in chemical mechanical polishing. J Electrochem Soc 156(10):408–412. doi:10.1149/1.3186032

31. Luo JF, Dornfeld DA (2003) Effects of abrasive size distribution in chemical mechanical planarization: modelling and verification. IEEE Tran Semicond Manuf 16(3):469–476. doi:10.1109/TSM.2003.815199

32. Uneda M, Maeda Y, Ishikawa K, Ichikawa K, Doi T (2012) Relationships between contact image analysis results for pad surface texture and removal rate in CMP. J Electrochem Soc 159(2): 90–95. doi:10.1149/2.008202jes

33. Lu LY, Fang CF, Shen JY, Lu J, Xu XP (2014) Analysis of path distribution in lapping and polishing with single fixed abrasive. Key Eng Mater 589–590:475–479. doi:10.4028/www.scientific.net/KEM.589-590.475

34. Roswell A, Xi FF, Liu GJ (2006) Modelling and analysis of contact stress for automated polishing. Int J Mach Tools Manuf 46(3-4): 424–435. doi:10.1016/j.ijmachtools.2005.05.006

35. Dong ZC, Cheng HB (2014) Study on removal mechanism and removal characters for SiC and fused silica by fixed abrasive diamond pellets. Int J Mach Tools Manuf 85:1–13. doi:10.1016/j.ijmachtools.2014.04.008